Electronic Supplementary Material (ESI) for Sustainable Energy & Fuels.

Supporting Information

Iron foam acts as a substrate and iron source in-situ constructing robust transition metal phytate electrocatalyst for overall water splitting

Xiaojuan Chen[a], Yan Meng[a], Taotao Gao[a], Jinmei Zhang[b], Xiaoqin Li[c], Hongyan Yuan[a]* and Dan Xiao[abc]*

[a]*College of Chemical Engineering, Sichuan University, Chengdu 610064, PR China*

[b]Key Laboratory of Green Chemistry and Technology, Ministry of Education, College of Chemistry, Sichuan University, Chengdu 610064, PR China

[c]*Institute of New Energy and Low-Carbon Technology, Sichuan University, Chengdu 610065, PR China*

*Corresponding Authors E-mail: xiaodan@scu.edu.cn; yuan_hy@scu.edu.cn

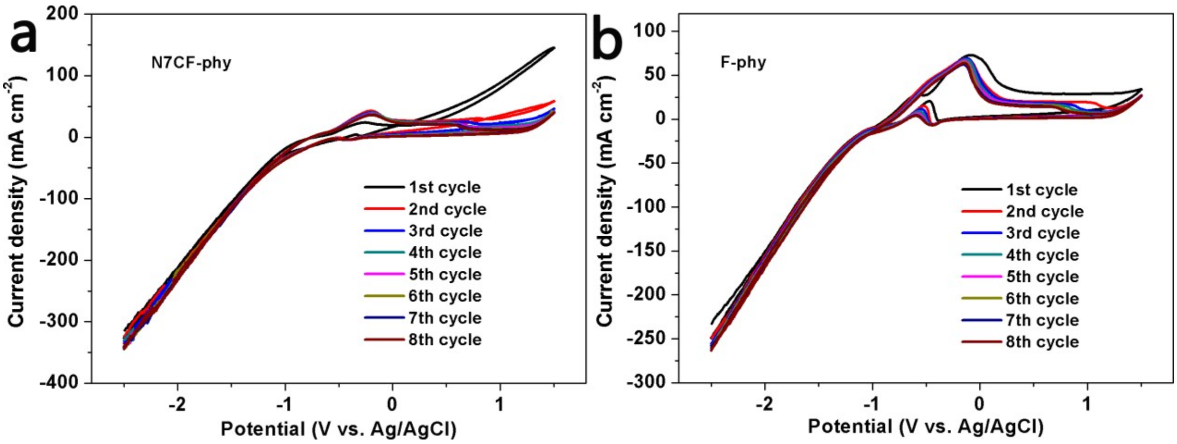

Fig. S1 The electrochemical preparation processes of N7CF-phy (a) and F-phy (b).

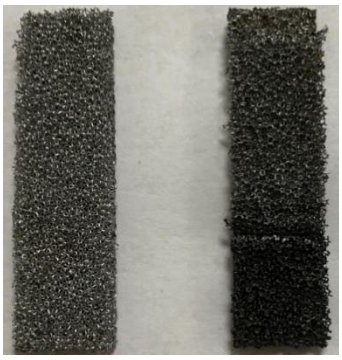

Fig. S2 The photographs of bare IF and N7CF-phy.

Table S1 Some physical properties of the bare IF and the N7CF-phy. The interfacial contact area is estimated with the electrochamical active surface area in Fig. S9 and the charge transfer resistance is corresponding to the conductivity. The corresponding fitted data and equivalent circuit diagram are shown in Fig. S3.

Electrodes	Porosity	Electrochemical Active Surface Area	Rct (Charge Transfer Resistance) (Ω)
IF	60%	1.382 mF cm^{-2}	158
N7CF-phy	~60%	7.798 mF cm^{-2}	0.5

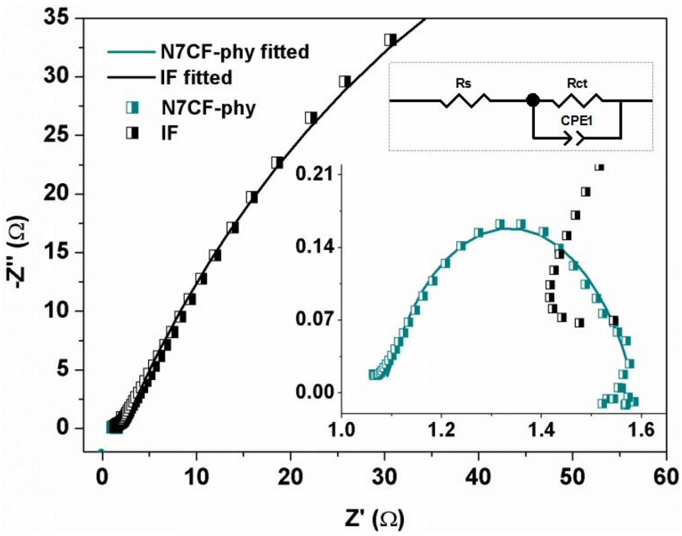

Fig. S3 The EIS data and their fitting data of the N7CF-phy and bare IF electrodes.

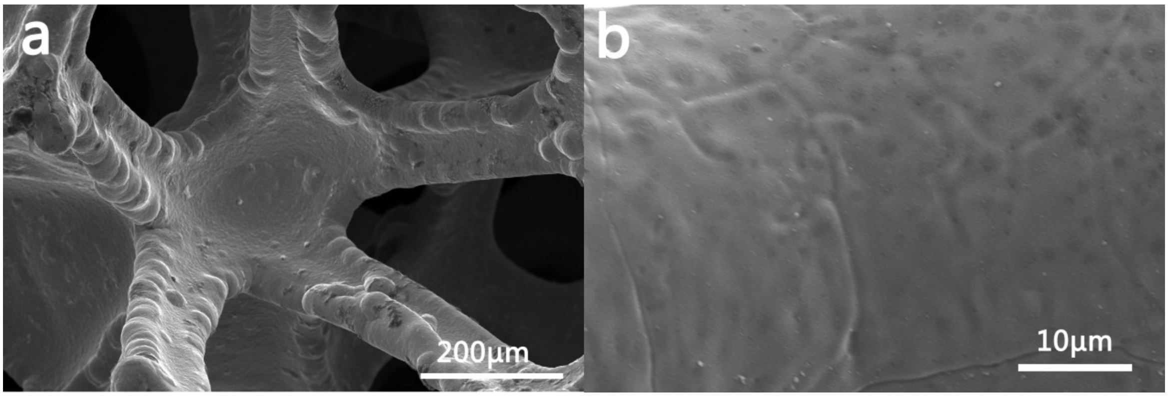

Fig. S4 The SEM images of F-phy .

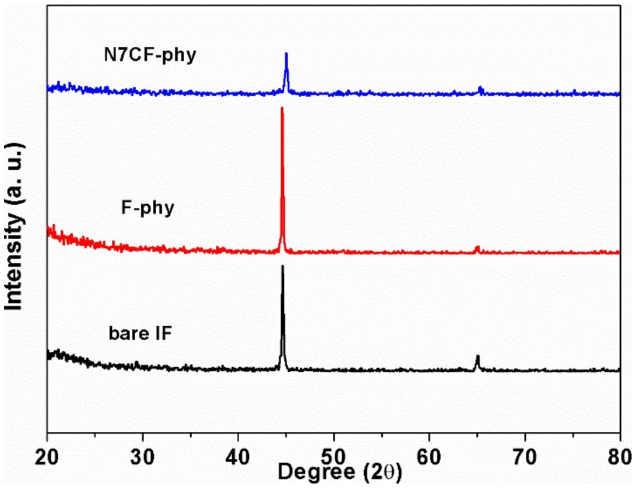

Fig. S5 XRD images of the electrodes.

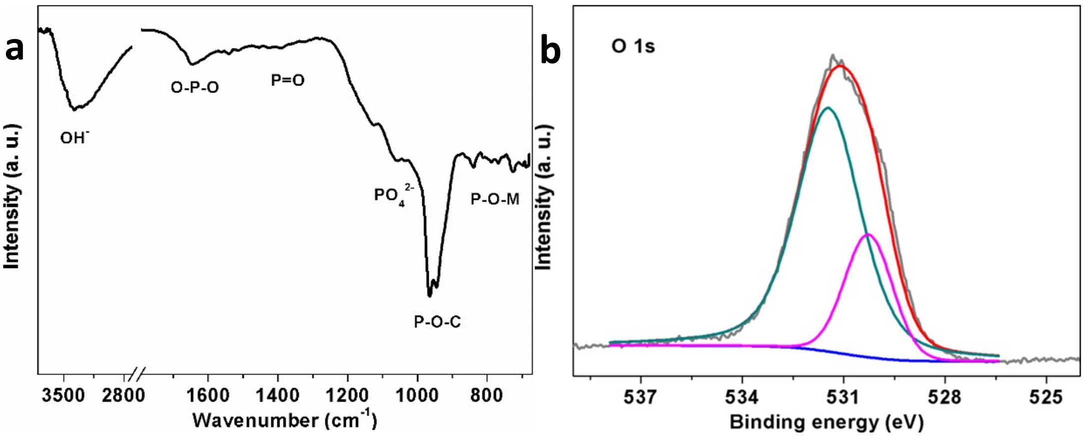

Fig. S6 (a) ATR-IR spectrum and the (b) O1s XPS image of N7CF-phy.

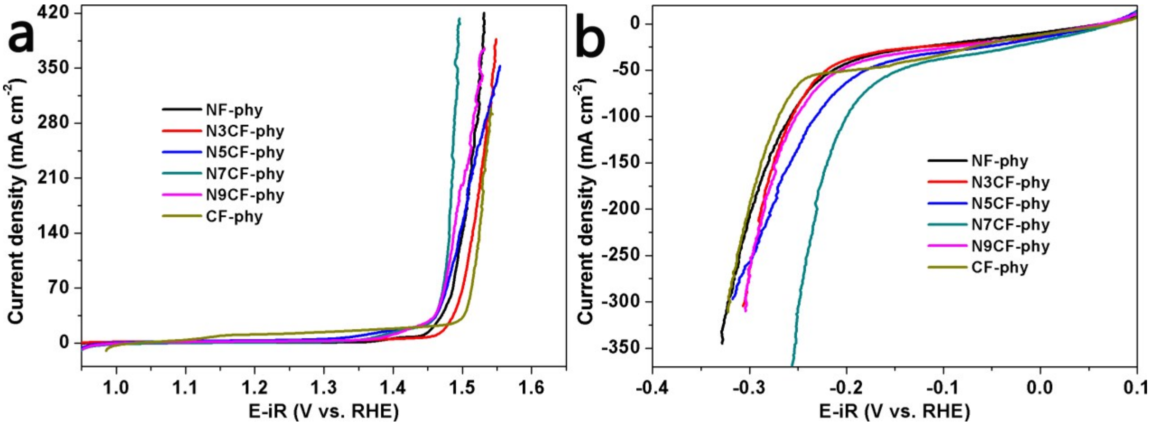

Fig. S7 The OER and HER performances of electrodes.

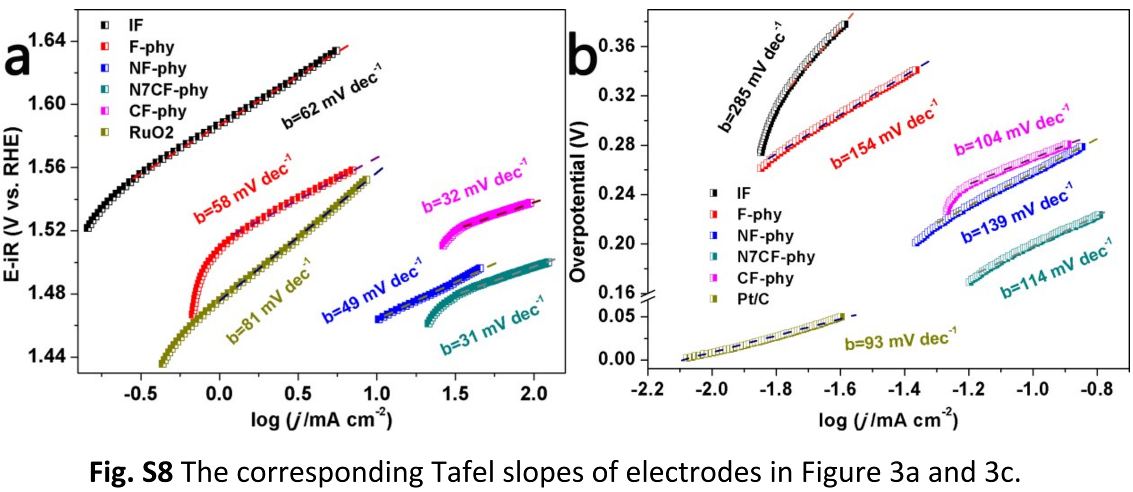

Fig. S8 The corresponding Tafel slopes of electrodes in Figure 3a and 3c.

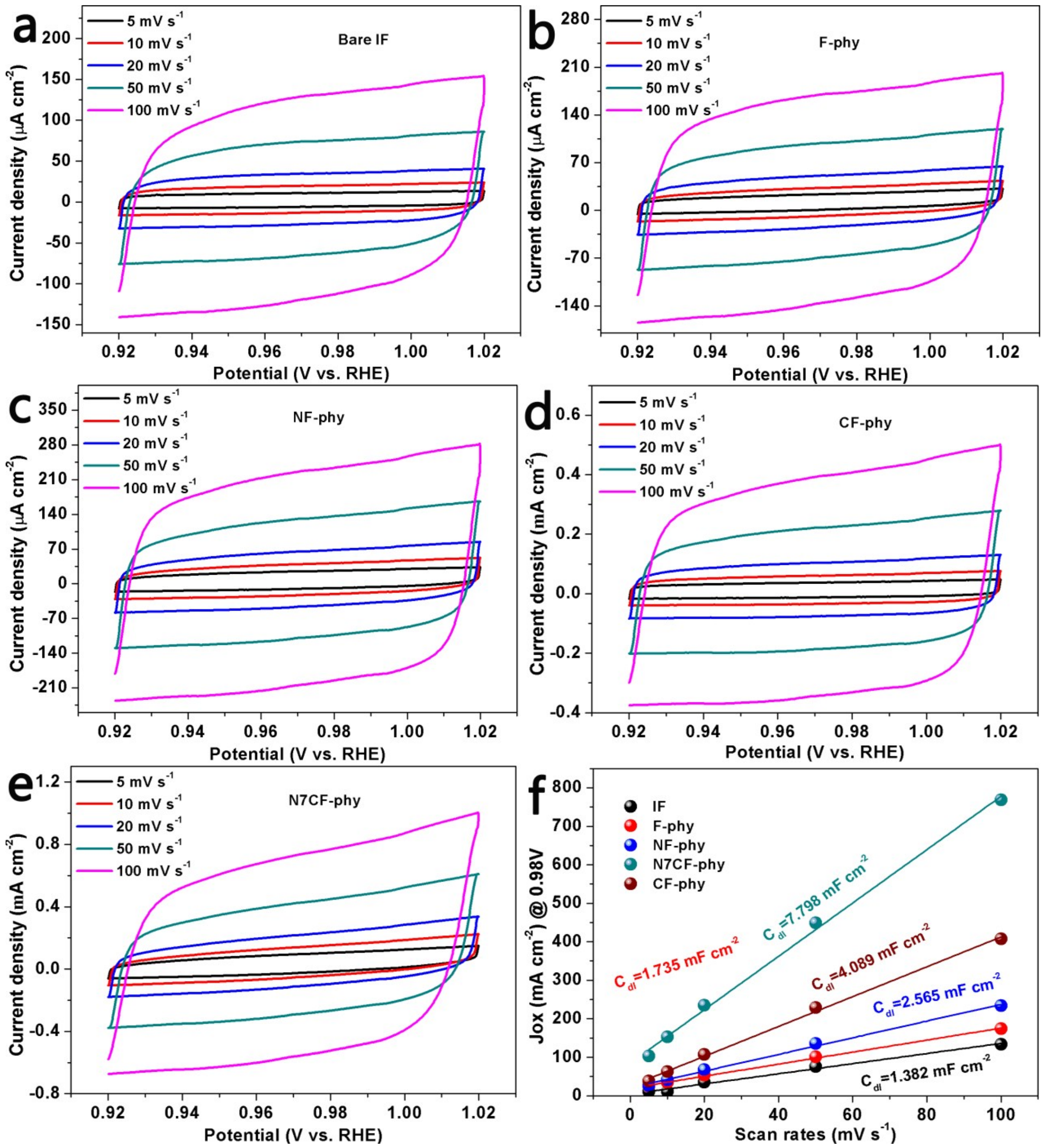

Fig. S9 Electrochemical double-layer capacitance measurements of various electrodes at the scan rates of 5, 10, 20, 50 and 100 mV s^{-1} in 1 M KOH and the linear fitting curves of the charged currents at 0.98 V of each electrode vs. scan rates.

The calculation of faradaic efficient:

At first, the chronopotentiometric measurement was applied to the three-electrode system, with the gas-collecting method to gather the volume of the generated O_2 and H_2 in saturated solution of oxygen. The state equation of gas (PV=nRT, normal temperature and pressure) was used to obtain the molar of actual gas. Comparing to the theoretical gas yield, the corresponding faradaic efficient image is shown in Fig. S10.

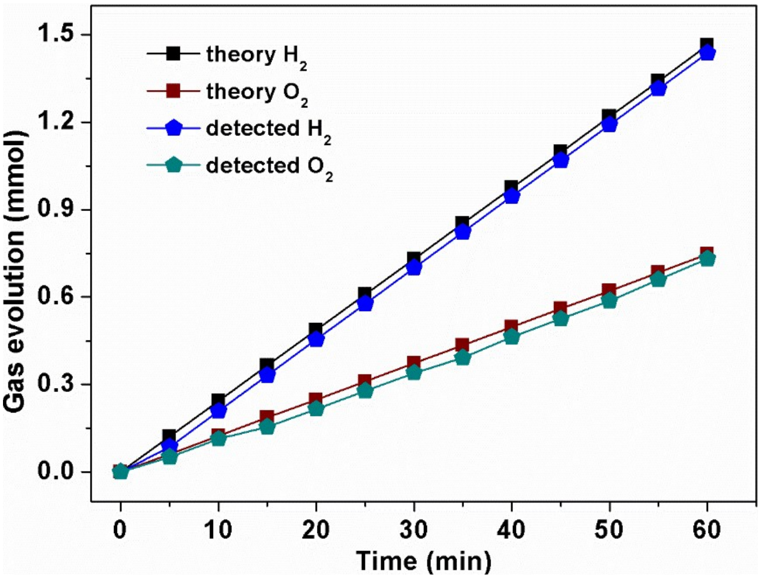

Fig. S10 Faradaic efficient of the electrode at a constant current density of ±80 mA cm^{-2} in 1.0 M KOH.

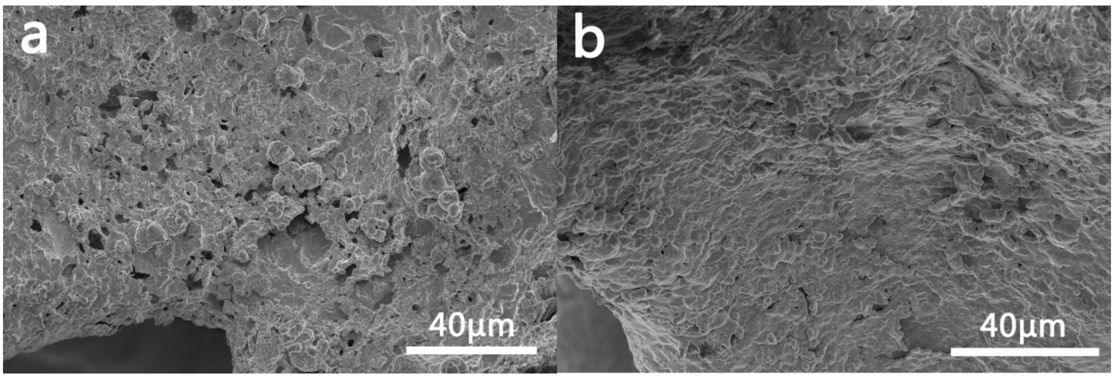

Fig. S11 (a,b) SEM images of N7CF-phy after OER and HER stability measurement.

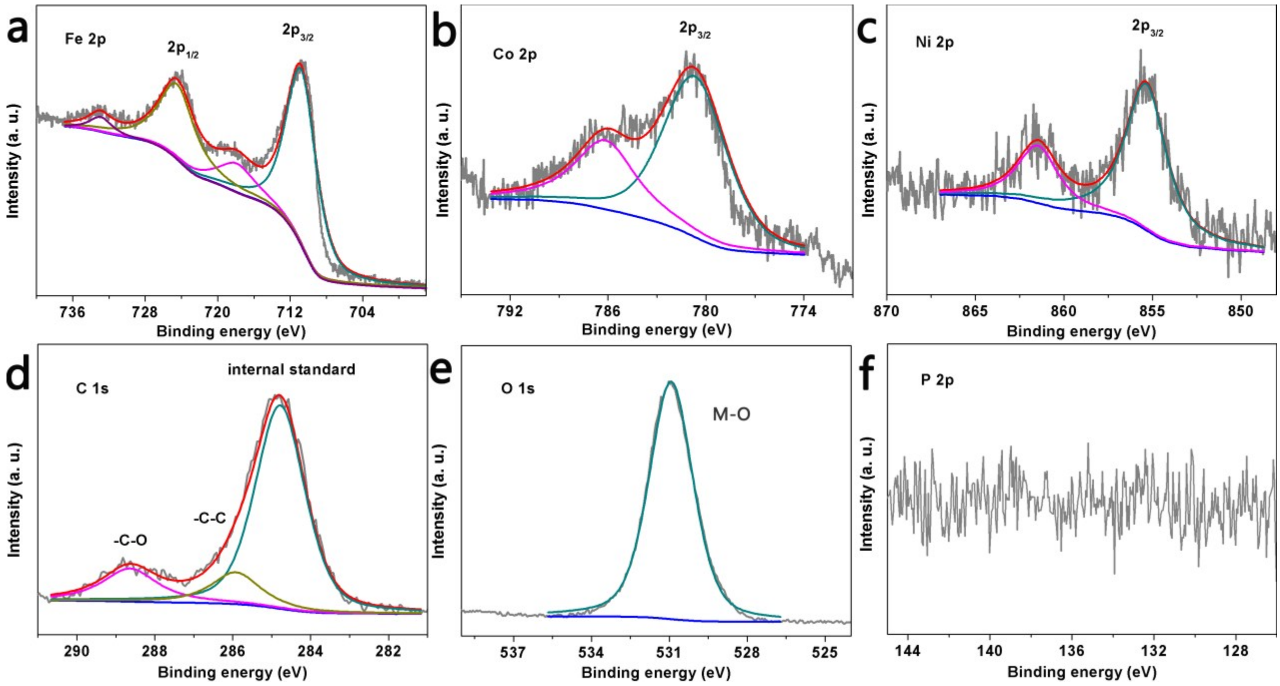

Fig. S12 (a-g) XPS images of N7CF-phy after OER stability measurement.

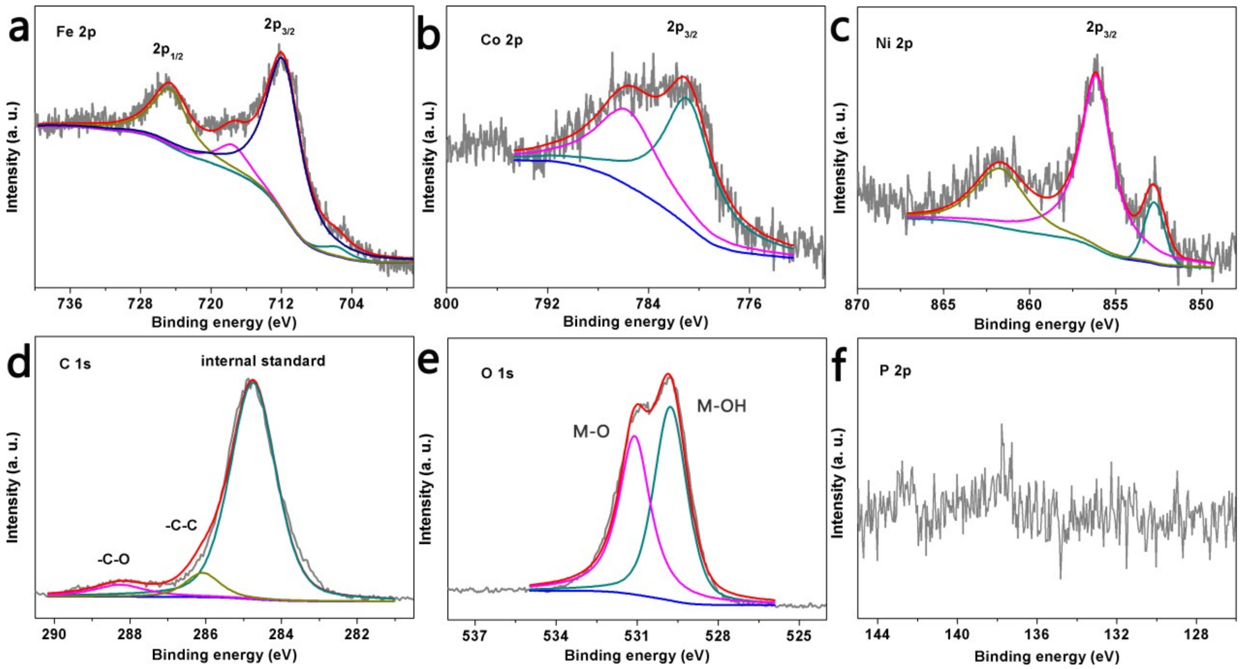

Fig. S13 (a-g) XPS images of N7CF-phy after HER stability measurement.

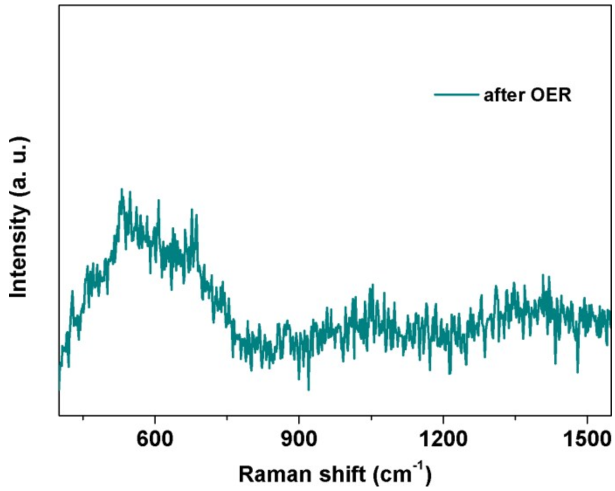

Fig. S14 The Raman spectra of N7CF-phy after OER durability.

After OER durability, the peaks at 474 and 554 cm^{-1} corresponding to NiOOH. [1] Fe_2O_3 peak located at 508 and 606 cm^{-1}, and the peaks at 661 and 690 cm^{-1} belong to FeOOH species.[2] The peaks at 480 cm^{-1}, 617 cm^{-1} and 687 cm^{-1} are corresponding to Co_3O_4.[3] A broad peak in the region of 900~1200 cm^{-1} is assigned to ν(O−O) of an active oxygen species MOO−.[4]

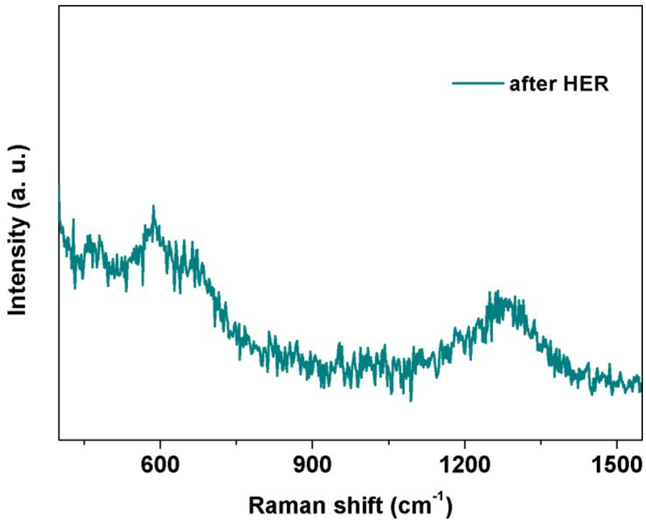

Fig. S15 The Raman spectra of N7CF-phy after HER durability.

After HER durability, The peaks at 479 and 555 cm^{-1} are assigned to M-O species of NiOOH species, and the peaks at around 592 cm^{-1} belong to vibration of Ni(OH)2, and around 515 cm^{-1} belongs to $Fe(OH)_3$. [2,4,5] The peaks at 488 cm^{-1}, 618 cm^{-1} and 661 cm^{-1} belong to $Co3O_4$. [6]

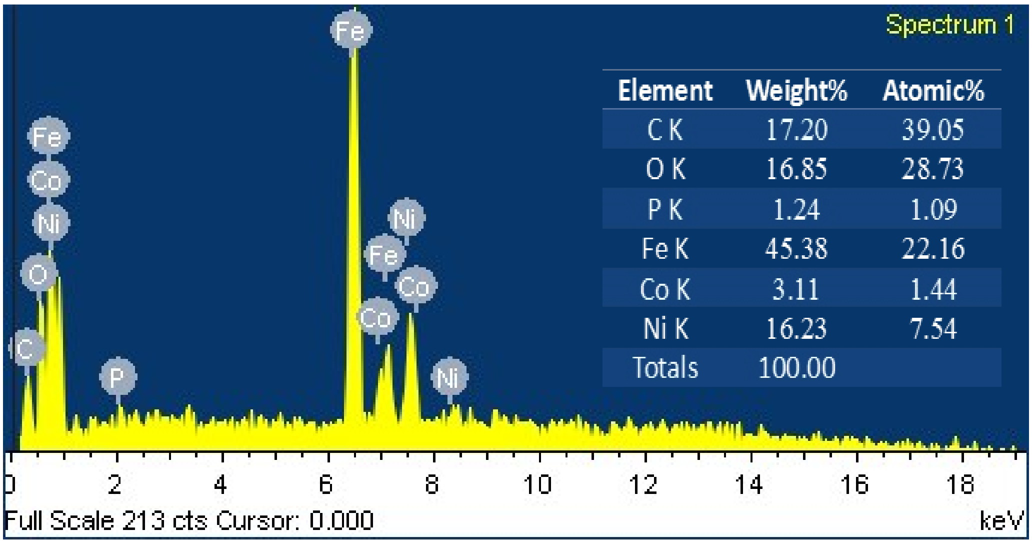

Fig. S16 The EDS pattern of N7CF-phy after OER durability.

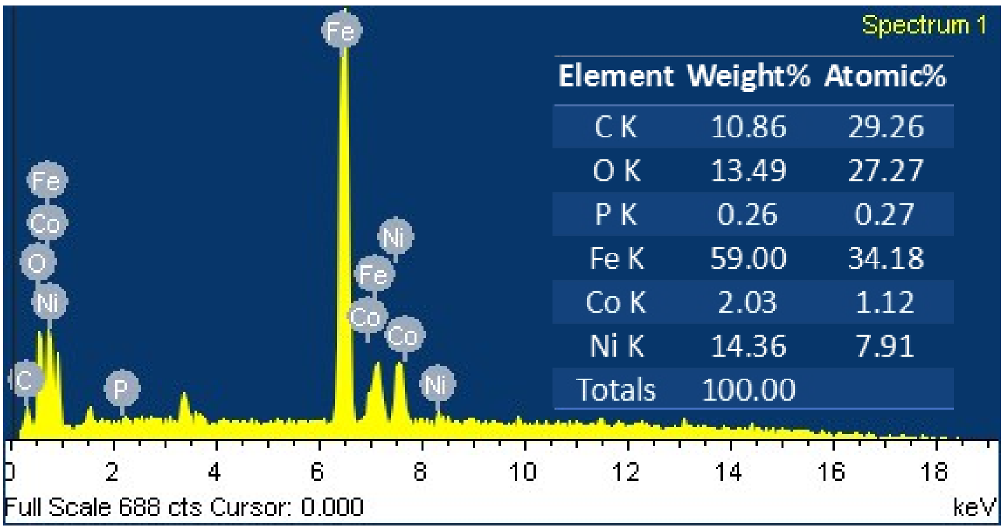

Fig. S17 The EDS pattern of N7CF-phy after HER durability.

Table S2. Comparisons of the various OER catalysts in 1 M KOH according to the reports and this paper.

Catalysts	Substrate	Tafel slope	Current density (J, mA cm^{-2})	η at corresponding J (mV)	Stability	Ref
NiCo-LDH	Carbon paper	40	10	367	An increase of 22 mV after 6 hours' electrocatalysis at 10 mA	7
Ni/Ni_3N	NF	60	10	~322	~ 96% current density retention after 12 hours' electrocatalysis at 100 mA cm^{-2}	8
NiFe	NF	28	80 100	270 370	~ 100% current density retention after 10 hours' electrocatalysis at 100 mA cm^{-2}	9
NiS	NF	89	50	335	~ 100% current density retention after 35 hours' electrocatalysis at 13 mA cm^{-2}	10
NiSe	NF	64	100	314	~ 99% current density retention after 12 hours' electrocatalysis at 100 mA cm^{-2}	11
$Ni_{1.5}Fe_{0.5}P$	Carbon paper	55	10 20	264 280	current density almost unchanged after 1000 cycles	12
NiFe-P	NF	88	20 200	204 376	η even lower than the initial value after 12 h galvanostatic catalysis	13
NiP	NF	23	191	350	From 1.33V gradually increases to 1.45 V vs. RHE after 0.2 h, and then remains fairly stable at this potential up to 26 h	14
MoP	NF	56.6	10	265	After 1000 continuous CV cycles, the polarization curve only deviates slightly from the initial one	15
NiFeP	NF	87	10	280	slightly increases from 1.51 to 1.53 V versus RHE after 24 h at 10 mA cm^{-2}	16
N7CF-phy	IF	31	20 100 200	224 267 275	99% current density retention after 66 and 22 hours' electrocatalysis at 500 and 100mA cm^{-2}	This work
F-phy	IF	58	100 200	399 409	~ 98% current density retention after 20 hours' electrocatalysis at 100 mA cm^{-2}	This work

Table S3. Comparisons of the various HER catalysts in 1 M KOH according to the reports and this paper.

Catalyst	Substrate	Current density (J, mA cm^{-2})	η at corresponding J (mV)	Reference
NiS	NF	20	158	10
NiSe	NF	50	182	11
$Ni_{2.3\%}$-CoS_2	Carbon cloth	100	231	17
$Ni_{1.5}Fe_{0.5}P$	Carbon paper	10	282	12
NiFe-P	NF	200	355	13
MoP	NF	10	390	15
N7CF-phy	IF	50 100 200	145 200 229	This work
F-phy	IF	50 100	350 390	This work

Table S4. Comparisons of the two-electrode configuration performance according to the reports and this paper in 1 M KOH.

Catalyst	Substrate	η@10 mA cm^{-2} (mV)	Current density (J, mA cm^{-2})	η at corresponding J (mV)	Reference
$FeNi_3N$	NF	390	～90	770	18
NiP	NF	410	100	820	14
NiSe	NF	400	～60	770	11
$NiCo_2S_4$ NW	NF	400	～70	770	19
$Ni_{1.5}Fe_{0.5}P$	Carbon paper	-	20	493	15
CP@Ni-P	Carbon paper	400	20	500	20
N7CF-phy	IF	320	20 100	460 710	This work

References:

1. Li, Y., Hu, L., Zheng, W., Peng, X., Liu, M., Chu, P., Lee, L. Y., *Nano Energy*, 2018, 52, 360-368.
2. Cheng, X., Pan, Z., Lei, C., Jin, Y., Yang, B., Li, Z., Zhang X., Lei L., Yuan, C., Hou, Y., *J. Mater. Chem. A*, 2019, 7(3), 965-971.
3. Li, X., She, F., Shen, D., Liu, C., Chen, L., Li, Y., Zhao D., Chen Z., Wang, H., *RSC Adv.*, 2018, 8(50), 28625-28631.
4. Lee, S., Banjac, K., Lingenfelder, M., Hu, X., *Angew. Chem., Int. Ed.* 2019
5. Liu, Y., Jin, Z., Tian, X., Li, X., Zhao, Q., Xiao, D. *Electrochim. Acta,* 2019
6. Islam, M., Zuba, M., DeBiase, V., Noviasky, N., Hawley, C., *Nanotechnology*, 2018, 29(7), 075403.
7. Liang H., Meng F., Cabán-Acevedo M., Li L., Forticaux A., Xiu L., Wang Z., Jin S., *Nano Letters*, 2015, 15, 1421-1427.
8. Shalom M., Ressnig D., Yang X., Clavel G., Fellinger T. P., Antonietti M., *J. Mater. Chem. A*, 2015, 3, 8171-8177.
9. Lu X., Zhao C., *Nature Commun.*, 2015, 6, 6616..
10. Zhu W., Yue X., Zhang W., Yu S., Zhang Y., Wang J., Wang J., *Chemical Commun.*, 2016, 52, 1486-1489.
11. Tang C., Cheng N., Pu Z., Xing W., Sun X., *Angew. Chem., Int. Ed.*, 2015, 54, 9351-9355.
12. Huang H., Yu C., Zhao C., Han X., Yang J., Liu Z., Li S., Zhang M., Qiu J., *Nano Energy*, 2017, 34, 472-480.
13. Xing J., Li H., Cheng M., Geyer S., Ng K., *J. Mater. Chem. A*, 2016, 4, 13866-13873.
14. Wang X., Li W., Xiong D., Liu L., *J. Mater. Chem. A*, 2016, 4, 5639-5646.
15. Jiang Y. , Lu Y., Lin J., Wang X., Shen Z., *Small Methods*, 2018, 2(5), 1700369.
16. Liang H., Gandi A. N., Anjum D. H., Wang X., Schwingenschlögl U.,. Alshareef H. N, *Nano letters*, 2016, 16, 7718-7725.
17. Fang W., Liu D., Lu Q., Sun X., Asiri A. M., *Electrochem. Commun.*, 2016, 63, 60-64.
18. Zhang B., Xiao C., Xie S., Liang J., Chen X., Tang Y., *Chem. Mater*, 2016, 28, 6934-6941.
19. Sivanantham A., Ganesan P., Shanmugam S., *Adv. Funct. Mater.*, 2016, 26, 4661-4672.
20. Wang X., Li W., Xiong D., Petrovykh D. Y.,Liu L., *Adv. Funct. Mater.*, 2016, 26, 4067-4077.